Short communication

Sulfonated polyimide/PTFE reinforced membrane for PEMFCs

L. Wang [a,b], B.L. Yi [a,*], H.M. Zhang [a], Y.H. Liu [a,b], D.M. Xing [a],
Z.-G. Shao [a], Y.H. Cai [a,b]

[a] *Proton Exchange Membrane Fuel Cell Key Materials and Technology Laboratory, Dalian Institute of Chemical Physics,*
Chinese Academy of Science, 457 Zhongshan Road, Dalian, Liaoning 116023, PR China
[b] *Graduate School of the Chinese Academy of Sciences, Beijing 100039, PR China*

Abstract

A sulfonated polyimide (SPI)/PTFE reinforced membrane was synthesized by impregnating PTFE (porous polytetrafluoroethylene) membrane with a SPI/DMSO solution. The resulting composite membrane was mechanically durable and quite thin relative to traditional perfluorosulfonated ionomer membranes (PFSI). We expect the PTFE to restrict the swelling and dimensional change of the SPI when it is immersed into water. And the reinforcement with PTFE can increase the hydrolysis stability of the SPI due to the low swelling and low dimensional change. From ex-situ testing and a short term fuel cell "life" test, we conclude that the PTFE reinforced sulfonated polyimide had a higher hydrolytic stability than pure sulfonated polyimide. The thin SPI/PTFE membrane showed comparable fuel cell performance with the commercial NRE-212 membrane with H_2/O_2 at 80 °C under fully humidified conditions. The chemically modified membrane with Nafion layer showed good stability in a 120 h fuel cell test.
© 2007 Elsevier B.V. All rights reserved.

Keywords: PEMFC; Composite membrane; Sulfonated polyimide; Nafion; Multilayer

1. Introduction

Fuel cells are efficient devices to generate electric power via electrochemical reaction of fuels with oxygen and therefore have attracted attention as a clean powering system [1]. However, the cost of the cell components precludes their immediate implementation for most stationary and vehicular applications. One of the contributors to the PEM fuel cell's high cost is the perfluorosulfonated ionomer membrane (PFSI). Also the high gas permeability and environmental inadaptability of the fluorinated materials are serious drawbacks for the practical fuel cell applications.

Alternative low cost membranes with improved properties are thus needed and many different kinds of membranes have been investigated during the last ten years [2–4]. These membranes are mainly sulfonated aromatic thermostable polymers such as polyetherketones, polysulfones, polyparaphenylenes

or polybenzimidazoles. Sulfonated polyimides (SPI) based on naphtahalenic moieties are considered to be promising materials owing to their swelling, mechanical and conducting properties [5]. Despite the above-mentioned salient properties, the hydrolytic stability is a primary obstacle for the application as electrolyte membrane in a fuel cell. Various approaches have been put forth to develop membranes with higher hydrolytic stability that include: (1) incorporating monomers having flexible linkages [6]; (2) incorporating monomers not having both sulfonic acid group and amine group in the same ring [7]; (3) diamine monomers having high nucleophilicity [8]; (4) using aliphatic diamines [9]; (5) using napthalenic dianhydrides [10]; and (6) diamines having sulfonic acid group in side chain [11]. For preparing more stable membranes, a method of reinforcement was developed to increase the stability of hydrocarbon membranes. For example, Xing and co-workers used porous polytetrafluoroethylene (PTFE) to reinforce SPEEK [12] and Yamaguchi used porous PTFE as a porous substrate and filled the pores with poly (vinylsulfonic acid/acrylic acid) crosslinked gel. The composite membrane had a low methanol permeability and was thermally stable to 130 °C [13]. In our previous work,

---

we used the porous PTFE membrane to reinforce the Nafion [14]. The mechanical stability and maximum strength of the membrane were improved. The good tensile strength made it possible for a thinner composite membrane to be used in the fuel cell which improves the cell performance.

In this article, we report a method to reinforce the SPI with porous PTFE. The swelling and mechanical stability were improved for the composite membrane. Therefore, the reinforced structure improved the stability of the membrane operating in fuel cell conditions. The chemically modified composite membrane with two Nafion layers on the sides of the SPI/PTFE membrane, shows good stability due to the reinforcement of the PTFE and the chemical stability of the Nafion.

2. Experimental

2.1. Membrane preparation

The 10 μm porous PTFE support films (manufactured in Shanghai DaGong New Materials Co Ltd., China) with pore diameter 0.3–0.5 μm and thickness 10 μm were first cleaned by soaking in ethanol for 30 min at room temperature, and then dried in an oven at room temperature. They were then extended over a flat glass plate, the DMSO solution of SPI (NTDA-BDSA/ODA (1/1), IEC = 1.98 meq g^{-1}) in TEA salt form was then poured onto the PTFE films. The SPI used here was prepared by the same method reported previously [15]. The glass plate was dried on a hot plate at 75 °C for 24 h and finally dried in a vacuum oven at 120 °C for 12 h. In the process, gravity forced the SPI solution into the pores of the PTFE films. And after the evaporation of solvent, SPI was completely plugged, thus making the composite membranes air-tight. The thickness of the composite membranes was easily controlled by the amount of the SPI solution. The as-cast membrane was soaked in 0.5 M H$_2$SO$_4$ at room temperature for 12 h. The membrane was thoroughly washed with de-ionized water. The membrane thickness was about 25 μm.

The chemical modified SPI/PTFE membrane was prepared by immersing the SPI/PTFE membrane into the 5% Nafion® dispersion (Nafion® R-1100 resin, DuPont Fluoroproducts, USA). The coated membrane was dried in an oven at 60 °C for 12 h to remove the residual solvents and at 120 °C for 12 h to make the Nafion crystallization. The thickness of the Nafion/SPI-PTFE/Nafion membrane was about 30 μm.

2.2. Scanning electron microscope (SEM) and energy dispersive spectrum (EDS) study

A JEOL (JSM 6360LV SEM) microscope was used to observe the cross-sectional morphology of the composite membrane. Then, an Oxford Instruments X-ray Microanalysis 1350 was used to analyze the elemental distribution across the composite membrane. The composite membranes were cut in liquid nitrogen (77 K) to expose their cross-sections.

2.3. Electrochemical impedance spectroscopy (EIS) measurements

Proton conductivity was measured using a four-point probe electrochemical impedance spectroscopy technique over the frequency range from 10 Hz to 100 kHz (Princeton Applied Research PARSTAT 2273). The cell was placed in de-ionized water. The resistance value associated with the membrane conductance was determined from high-frequency intercept of the impedance with the real axis. Proton conductivity was calculated from the following equation:

$$\sigma = \frac{L}{RDW} \tag{1}$$

where L is the distance between the two reference electrodes, R the measured membrane resistance value, and D and W are the thickness and width of the sample membrane at the ambient conditions, respectively. The swollen membrane thickness was used in the calculation of σ.

2.4. Water uptake and swelling

Samples were weighed (W_1) after drying in a vacuum oven at 80 °C for 24 h. Then, Samples of the membranes were weighed (W_2) after immersion in deionized water for 12 h at 80 °C. Water content (ΔW) was calculated from Eq. (2).

$$\Delta W(\text{wt.\%}) = \frac{(W_2 - W_1)}{W_1 \times 100} \tag{2}$$

where W_1 and W_2 is the dry mass and wet mass of the sample expressed in gram, respectively.

Membranes specimens (size 4 cm × 5 cm) were stored in the a vacuum oven at 80 °C for 24 h and the distance between specified positions was measured before (L_1) and after (L_2) the samples were soaked in deionized water at 80 °C for 12 h. Dimensional change (ΔL) was calculated by using the following equation:

$$\Delta L(\%) = \frac{(L_2 - L_1)}{L_1 \times 100} \tag{3}$$

2.5. Water stability

The stability toward water of the SPI and SPI/PTFE membranes were examined by soaking the membranes in distilled water at 80 °C and was characterized by the expended time until the hydrated membranes lost their mechanical properties. The criterion for the judgment of the loss of mechanical properties was that the membrane was broken when lightly bent. Also the residual weight after being immersed in distilled water at 80 °C for 24 h was recorded for both the SPI and SPI/PTFE membranes. The membranes before and after the water stability test were examined by FTIR. The same weight of SPI and SPI/PTFE membranes were immersed into 60 mL distilled water in distilled water at 80 °C for 24 h. The soaking water solutions after the hydrolytic test of the SPI and SPI/PTFE membranes were examined by UV–vis. The UV–vis absorption spectra were recorded on an UV/vis spectrophotometer (JASCO, V-550). Fourier

transform infrared (FT-IR) absorption spectra were recorded on a JASCO FT/IR-4100 spectrometer from solution-cast films.

2.6. Tensile strength

Samples of the membranes were dried in a vacuum oven at 80 °C for 24 h for measuring of the tensile strength. The maximum strength was measured with a tension tester AG-2000A (Shimadzu, AUTOgraph) at room temperature. Tensile conditions were based on Chinese Standard QB-13022-91 and samples were measured using a programmed elongation rate of 50 mm min^{-1}.

2.7. Fuel cell stability study

For the durability test of the cells with 30 μm Nafion/SPI-PTFE/Nafion membranes, the cells were operated at a constant current density of 1000 mA cm^{-2} at 80 °C under fully humidified conditions. The flow rates of the inlet gases were kept at H$_2$ 40 mL min^{-1} and O$_2$ 80 mL min^{-1}. The voltage at 1000 mA cm^{-2} and the open-circuit voltage (OCV) were recorded.

2.8. Membrane electrode assembly preparation and single cell test

The membrane electrode assembly (MEA) was prepared by a hot pressing process. The 20 wt.% Pt/Vulcan XC-72 (Pt/C) catalyst from E-TEK, carbon paper from Toray, PTFE suspension and Nafion solution (DuPont) were used in the MEA preparation. The Pt/C catalyst loading of the anode and the cathode were both 0.5 mg Pt cm^{-2}. Two electrodes with effective area 5 cm^2 were hot-pressed onto a membrane to form a MEA. The MEA was mounted in a single cell with stainless steel end plates and stainless steel mesh flow field as current collectors. The flowing channel of the hardware was a stainless tube. The fuel cell performance was evaluated by I–V curves at 80 °C. The fuel and oxidant were fed in with co-flow. The flow rates of inlet gases were kept at H$_2$ 40 mL min^{-1} and O$_2$ 80 mL min^{-1}.

The fuel cell was started by increasing the cell temperature set point to 80 °C and raising the humidifier temperatures to their respective values. Similarly, the H$_2$ and O$_2$ pipeline temperatures were also maintained 5 °C higher than the humidifiers to prevent water condensation in the pipelines. All data were obtained at the following conditions: humidifier temperature $T_{H_2}/T_{O_2} = 80/80$ °C; cell temperature $T_{cell} = 80$ °C; gas pressure $P_{H_2}/P_{O_2} = 0.30/0.30$ MPa. And the data were recorded after 12 h fuel cell operation.

3. Results and discussion

3.1. SEM and EDS study

The SEM photomicrograph of the cross-section of the composite SPI/PTFE membrane is shown in Fig. 1. We can see that there are not obvious PTFE pores in the cross-section of the
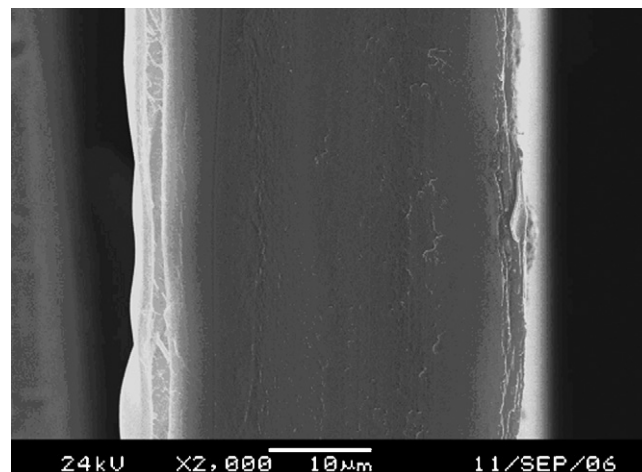

Fig. 1. SEM photomicrograph of the cross-section of the SPI/PTFE membrane.

SPI/PTFE membrane. Therefore, we conclude that the pores of the porous PTFE membrane are fully impregnated by the SPI resin. And the SPI is distributed uniformly in the composite membrane and completely plug the micropores.

Fig. 2 shows the EDS results of the cross-section of SPI/PTFE membrane. It can be seen that the S elements were dispersed asymmetrically along the cross-section of the membrane (Fig. 2a). This means that the SPI resin located on the PTFE side was less than the SPI resin located on the right side. From the EDX analysis results for the F element (Fig. 2b), the porous
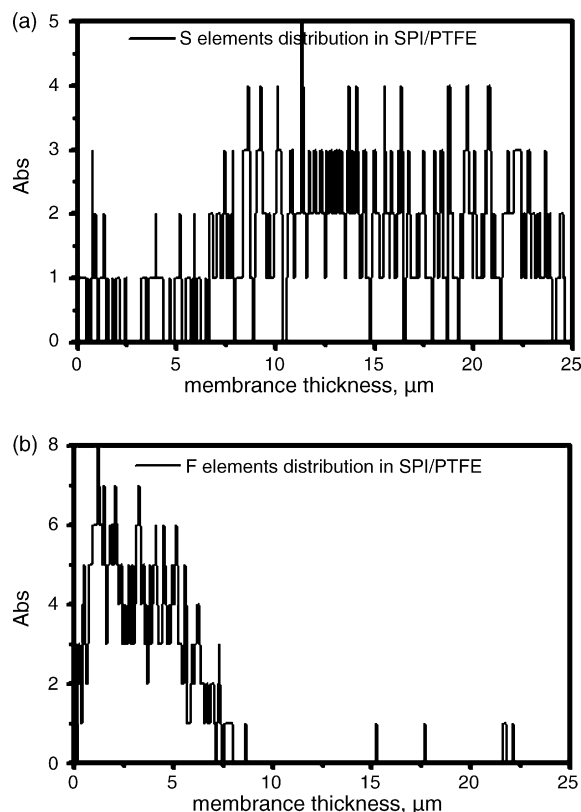

Fig. 2. EDS analysis results of SPI/PTFE membrane (cross-section), S element (a); F element (b).

Table 1
Water uptake, swelling and hydrolytic stability of the SPI/PTFE membranes and Nafion® NRE-212 membranes at 80 °C

Type of membranes	Water uptake (%)	Swelling (%)		Residue (wt.%)	Water stability (h)	Tensile strength (MPa)
		Thickness	Length			
SPI	45.2	55.6	7.1	85.3%	12	24.0
SPI/PTFE	33.3	31	1.5	98.6%	>50	30.5
NRE-212	26.2	20.5	25.2	100%	–	24.0

PTFE film was asymmetrically positioned in the composite membrane, and the SPI layers on each side of it. This is due to the gravitation of the PTFE, which is located at the bottom of the membrane when it is being prepared by the solution casting method.

3.2. Water uptake, swelling and hydrolytic stability study of the membranes

Table 1 shows the comparison of the water uptake and swelling of SPI/PTFE membrane and NRE-212 at 80 °C. The water uptake of SPI and SPI/PTFE membranes are obviously higher than the NRE-212 membrane. This is because the IEC of the SPI we used is about 1.98 meq g^{-1}, and it is higher than the IEC of NRE-212. The swelling of the SPI and SPI/PTFE shows anisotropy of the SPI induced by the rigidity of the SPI polymer chains [16]. The swelling of the SPI is reduced by the PTFE by about 50% and 80% for the length and thickness, respectively. The extreme swelling and dimensional change is one of the reasons caused the fail of the membrane in fuel cell. On the other hand, the sorption of a large amount of water will bring polymer chain relaxation, leading to significant loss in tensile strength. Here the porous PTFE reduced the swelling and the dimensional change greatly. The tensile strength is also increased by introducing PTFE to reinforce the SPI. The hydrolytic stability of the SPI/PTFE membrane is better than the SPI membrane by measuring the residual weight of the membranes after being immersed in water at 80 ° for 24 h and by comparing the time of breaking of the membranes when being lightly bent at 80 °C in

distilled water. All of these are expected to improve the stability of the membrane, and than increase the durability of the fuel cell.

The FT-IR spectrums of the membranes are shown in Fig. 3. The peaks at 1714 cm^{-1} and 1670 cm^{-1} are due to the naphthalimide absorption of the polyimides and peak at 1350 cm^{-1} represent the C–N vibration. The peak at 1499 cm^{-1} is due to the ether bridge absorption. The peaks at 1030 cm^{-1} and 1098 cm^{-1} are due to the stretching vibration of the SO$_2$ [17]. The peak at 1158 cm^{-1} is due to the stretching of the CF$_2$. The FT-IR spectra of SPI and SPI/PTFE membranes are compared between before and after the aging in water. We detected that the peak at 1670 cm^{-1} of the SPI membrane obviously changed to two peaks after hydrolyzation (Fig. 3, a and b). But the peak at 1670 cm^{-1} of the SPI/PTFE membrane changed little (Fig. 3, c and d). The split of the peak is due to the degradation of the naphthalimide of the sulfonated polyimide. So we concluded that reinforcement of the PTFE could slow the degradation of the SPI. The IR results suggest that the PTFE has the function of slowing the hydrolyzation of the SPI membrane.

Fig. 4 shows the UV spectrums after the hydrolytic test of SPI and SPI/PTFE membranes in water at 80 °C for 24 h. The two peaks at 385 nm and 364 nm and one shoulder around 340 nm are attributed to the naphthalenic components [18]. Because we immersed the SPI and SPI/PTFE membranes with the same weight into 60 mL distilled water, the UV absorbance of the soaking water can reflect the degradation rate of the membranes. The results show that the SPI/PTFE membrane had better hydrolytic stability than the SPI membrane.
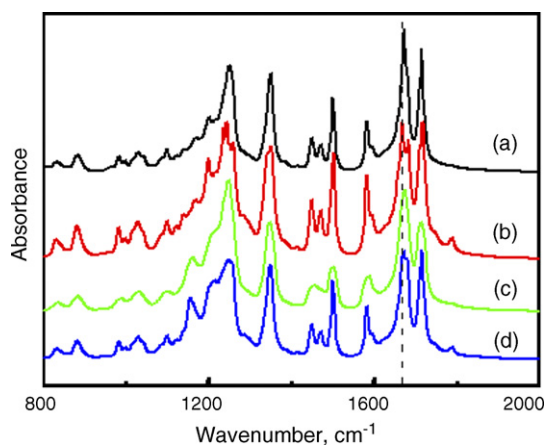

Fig. 3. FTIR spectra of the (a) SPI; (b) SPI (after aging); (c) native SPI/PTFE; and (d) SPI/PTFE (after aging).
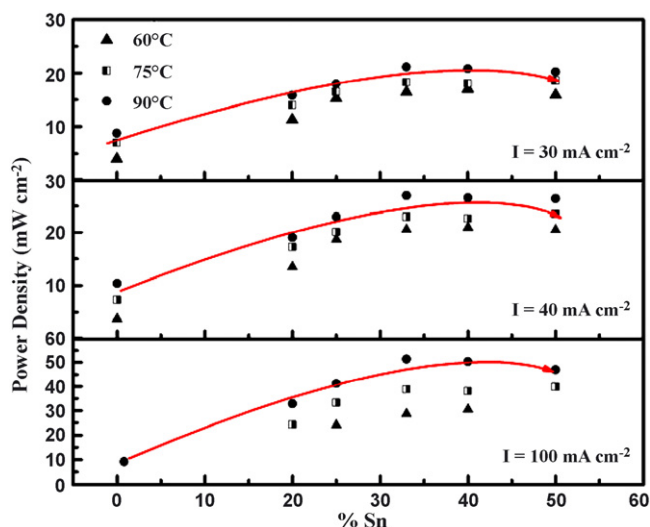

Fig. 4. UV spectra after the aging of SPI membrane and SPI/PTFE membranes.
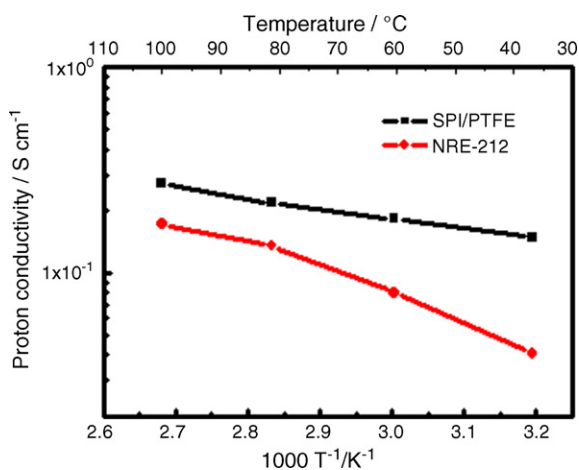
Fig. 5. Proton conductivities of the SPI membrane and NRE-212 membranes immersed in liquid water as a function of temperature.

Fig. 7. Fuel cell stability test of a single cell with Nafion/SPI-PTFE/Nafion membranes with fully humidified H_2/O_2 at 80 °C. $P_{H_2}/P_{O_2} = 0.30/0.30$ MPa.

3.3. Proton conductivities of the SPI/PTFE and NRE-212 membranes

Fig. 5 shows the proton conductivities of the SPI/PTFE and NRE-212 membranes immersed in liquid water. The results show that with the temperature increasing, the proton conductivities of the membranes increase. The proton conductivity of the SPI/PTFE membranes was higher than that of the NRE-212 membrane. Because the SPI/PTFE membrane was immersed into liquid water, the proton conductivity of the membranes was higher than the data reported in our previous reports [15]. The proton conductivities of the SPI/PTFE and NRE-212 membranes are similar to those reported in the literature [19].

3.4. Performance of PEMFCs operated under fully humidified conditions

Fig. 6 shows the polarization curves of cells with SPI/PTFE, Nafion/SPI-PTFE/Nafion and Nafion® NRE-212 membranes operated under fully humidified conditions with cell temper-
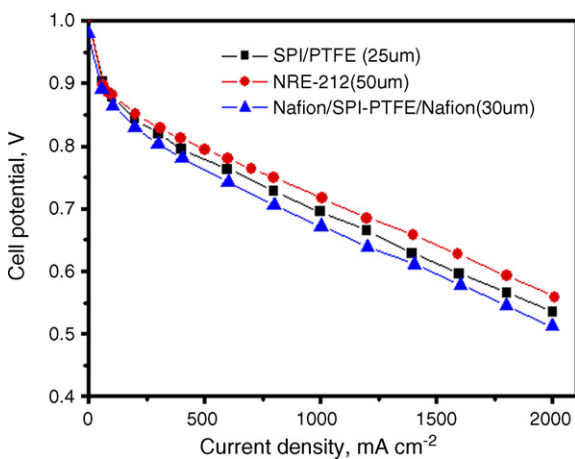

Fig. 6. Performance of H_2/O_2 fuel cells with SPI/PTFE, Nafion/SPI-PTFE/Nafion and Nafion® NRE-212 membrane under humidified conditions at 80 °C.
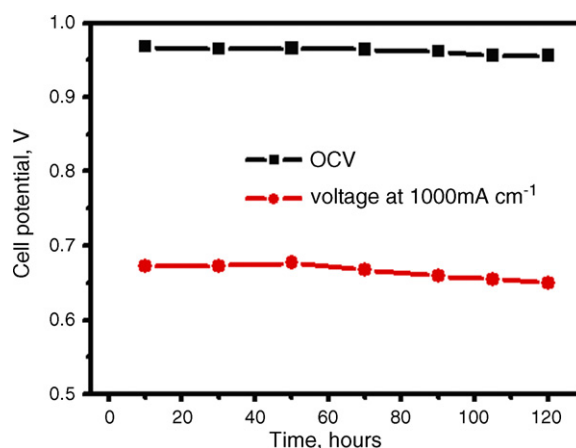
ature at 80 °C. The cell performance with the NRE-212 was better than that with the SPI/PTFE and Nafion/SPI-PTFE/Nafion membranes. The performance of the SPI/PTFE membrane was better than the Nafion/SPI-PTFE/Nafion membrane. In our previous work, the cell performance of SPI membrane was almost the same to the NRE-212 operated at this condition. The performance loss of the SPI/PTFE was due to the decrease of the proton conductivity of the membrane caused by the PTFE. The added two Nafion layers increased the membrane thickness, and therefore slightly affected the performance. However, the cell performances were still high compared to the commercial Nafion® NRE-212 membrane.

3.5. Durability test of the fuel cell

The voltage at the current density 1000 mA cm^{-2} and the OCV of PEM fuel cells with the Nafion/SPI-PTFE/Nafion composite membrane with time is shown in Fig. 7. It is found that there is no obvious decrease of the cell voltage at 1000 mA cm^{-2} and OCV of Nafion/SPI-PTFE/Nafion membranes at the time scale of experiment. From 50 h to 120 h, the cell voltage at 1000 mA cm^{-2} of Nafion/SPI-PTFE/Nafion membrane has a slightly decrease about 20 mV. However, the OCV of the fuel cell was still constant. These results were greatly improved compared to the results in our previous work [15]. It is suggested the PTFE reinforced SPI membrane has good stability under fuel cell conditions. The slight decrease may be due to the degradation of the proton conduction path in the SPI/PTFE membrane itself and/or at the interface between the SPI/PTFE membrane and the Nafion layer which might be responsible for an increase in the cell resistance.

Our data shows the increase in the stability of the membrane can resist the OCV decay rate of the fuel cell. These results provide a basis to the hypothesis that durability is also enhanced through improvements in dimensional stability, presumably due to a reduction of the impact of the shrinkage stresses developed in the membrane.

4. Conclusions

A SPI/PTFE reinforced membrane was prepared using SPI in a porous PTFE membrane. Because of the reinforcement of the PTFE, the dimensional stability and the tensile strength were greatly improved. The swelling of the membrane was reduced and the proton conductivity of the SPI/PTFE was higher than the NRE-212 membrane when they were immersed into liquid water. Using thin Nafion layers to modify the SPI/PTFE membrane the stability of the Nafion/SPI-PTFE/Nafion membrane was examined and verified by FT-IR, UV and short life time fuel cell test and compared to the results in our previous work. The cell performances with SPI/PTFE and Nafion/SPI-PTFE/Nafion composite membranes were comparable to that of Nafion® NRE-212.

Acknowledgment

References

[1] C.S. Kong, D.Y. Kim, H.K. Lee, Y.G. Shul, T.H. Lee, J. Power Sources 108 (2002) 185–191.
[2] O. Savadogo, J. New Mater. Electrochem. Syst. 1 (1998) 47–66.
[3] M. Rikukawa, K. Sanui, Prog. Polym. Sci. 25 (2000) 1463–1502.
[4] J. Rozie're, D. Jones, Annu. Rev. Mater. Res. 33 (2003) 503–505.
[5] N. Asano, M. Aoki, S. Suzuki, K. Miyatake, H. Uchida, M. Watanabe, J. Am. Chem. Soc. 128 (2006) 1762–1769.
[6] J. Fang, X. Guo, S. Harada, T. Watari, K. Tanaka, H. Kita, K. Okamoto, Macromolecules 35 (2002) 9022–9028.
[7] X. Guo, J. Fang, T. Watari, K. Tanaka, H. Kita, K. Okamoto, Macromolecules 35 (2002) 6707–6713.
[8] C. Lee, S. Sundar, J. Kwon, H. Han, J. Polym Sci. Part A: Polym. Chem. 42 (2004) 3621–3630.
[9] K. Miyatake, H. Zhou, H. Uchida, M. Watanabe, Chem. Commun. (2003) 368.
[10] C. Genius, R. Mercier, B. Sillion, R. Petiaud, N. Cornet, G. Gebel, M. Pineri, Polymer 42 (2001) 5097–5105.
[11] Y. Yin, J. Fang, Y. Cui, K. Tanake, H. Kita, K. Okamoto, Polymer 44 (2003) 4509–4518.
[12] L. Wang, D.M. Xing, Y.H. Liu, Y.H. Cai, Z.-G. Shao, Y.F. Zhai, H.X. Zhong, B.L. Yi, H.M. Zhang, J. Power Sources 161 (2006) 61–67.
[13] D.M. Xing, B.L. Yi, F.Q. Liu, Y.Z. Fu, H.M. Zhang, Fuel cells 3 (2005) 406–411.
[14] T. Yamaguchi, F. Miyata, S. Nakao, J. Membr. Sci. 214 (2003) 283–292.
[15] L. Wang, B.L. Yi, H.M. Zhang, Y.H. Liu, D.M. Xing, Z.-G. Shao, Y.H. Cai, J. Power Sources 164 (2007) 80–85.
[16] A.L. Rollet, O. Diat, G. Gebel, J. Phys. Chem. B. 108 (2004) 1130–1136.
[17] X.H. Ye, H. Bai, W.S.W. Ho, J. Membr. Sci. 279 (2006) 570–577.
[18] Y. Yin, Y. Suto, T. i Sakabe, S. Chen, S. Hayashi, T. Mishima, O. Yamada, K. Tanaka, H. Kita, K. Okamoto, Macromolecules 39 (2006) 1189–1198.
[19] Y. Yin, J.H. Fang, Y.F. Cui, K. Tanaka, H. Kita, K. Okamoto, Polymer 44 (2003) 4509–4518.